NUCLEAR
INSTRUMENTS
& METHODS
IN PHYSICS
RESEARCH
Section A

Radiation hardness of silicon detectors for future colliders *

E. Fretwurst, N. Claussen, N. Croitoru [1], G. Lindström, B. Papendick, U. Pein, H. Schatz,
T. Schulz and R. Wunstorf

I. Institut für Experimentalphysik, Universität Hamburg, Germany

The radiation hardness of silicon pad detectors, especially developed for the PLUG-calorimeter of the H1 experiment at HERA was investigated with respect to neutron and electron irradiation. Be(d, n)-neutrons with an average energy of 6.2 MeV up to a fluence of 10^{15} n/cm^2 and 1.8 MeV electrons up to a dose of 1 MGy (10^{16} e/cm^2) were used. Degradation effects of the diode properties regarding the reverse current, depletion voltage and charge collection efficiency are studied at room temperature and with no bias applied during irradiation. Special emphasis is put on the separation of the respective damage generation and its subsequent self annealing. The observed effects are discussed with respect to radiation levels to be envisioned for experiments with future colliding beam machines.

1. Introduction

The very intense radiation fields connected with the high luminosity of future colliding beam machines (LHC, SSC) make radiation hardness a most urgent demand for all detector components. As an example for a LHC luminosity of 10^{34} cm^{-2} s^{-1} an annual neutron fluence of up to 10^{14} n/cm^2 has been estimated in the forward region of a realistic detector configuration [1]. For the same pseudorapidity $\eta \approx 2.5$ the charged particle dose, dominated mainly by the electromagnetic component, is in the order of 10 kGy per year.

Radiation induced damage effects in silicon detectors can be roughly divided into two separate components. The dominant part is due to the bulk damage induced by the non-ionizing energy loss of the bombarding particles. In this respect neutron irradiation is much more effective leading to a much higher mean energy transfer to the primary knock on atom (PKA) than that by electrons. This is illustrated in fig. 1 showing the nonionizing energy loss (right scale) respectively the displacement cross section (left scale) as function of energy [2,3]. For example the ratio of the damage cross section for 1.8 MeV electrons to that of 1 MeV neutrons is about 10^{-2}.

In the following sections we describe results of our ongoing systematic investigations of radiation damage effects [4–8]. Degradation of the detector properties regarding the reverse current, depletion voltage, charge

collection efficiency and surface effects are studied at room temperature. Special emphasis is put on the separation of the respective damage generation and its subsequent self annealing. Only in this way it is possible to calculate the resulting effect during long term exposures under realistic operation conditions at future colliders [9,10]. Additional investigations referring also to damage effects at $-20°C$ and subsequent annealing at room temperature are included in the SITP report given at this conference [10].

2. Experimental technique

Numerous irradiation experiments were performed mainly with 6.2 MeV neutrons (from the Be(d, n) reaction) and 1.8 MeV electrons. The parameters of the different radiation fields are listed in table 1. High neutron intensities of 10^{10} n/cm^{2}s could be achieved by the Be(d, n)-source at a distance of 10 cm from the target. All measurements and calculations with respect to the neutron dosimetry were carried out by Brede et al. [11]. Details of the experimental setup and dosimetry for electron irradiations can be found in ref. [12]. All particle fluences were normalized to equivalent values for 1 MeV neutrons. In this way the trivial dependence of the observed damage on the nonionizing energy loss of different particles and energies is taken into account. For each radiation a corresponding hardness parameter κ was derived in such a way that $\Phi(E_n = 1 \text{ MeV}) = \kappa \Phi(E)$, where $\Phi(E)$ is the normal fluence for a given particle type and energy and $\Phi(E_n = 1 \text{ MeV})$ is the equivalent 1 MeV neutron fluence leading to the same nonionizing energy loss. The κ-val-
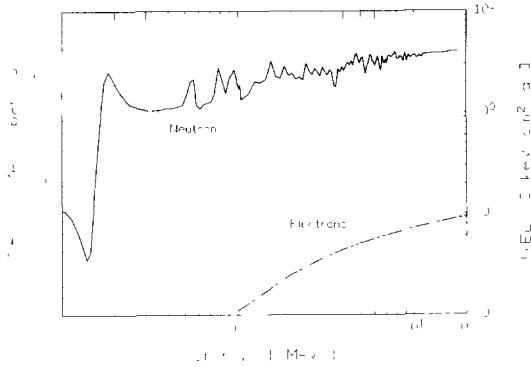
Fig. 1 Displacement damage cross section (left scale) resp. nonionizing energy loss NIEL (right scale) for neutrons [2] and electrons [3] as function of energy.

ues for neutrons were calculated using the damage cross sections of ref. [2] and for the case of electrons we used the nonionizing energy loss from ref. [3] (see table 1).

The silicon detectors used in our investigations are mainly of the planar-surface barrier-type. They were fabricated in our own laboratory from high resistivity (6 kΩ cm) n-type material (Wacker–Chemitronics) with a thickness of 400 μm. Different geometries of rectifying contacts with areas between 0.2 and 2 cm^2 were used in order to study possible edge effects. As outlined in a previous paper [4] the front electrode (Au) overlaps the SiO$_2$ edge protection layer, forming a narrow field plate which acts like a MOS-capacitor connected in parallel to the diode junction.

3. Change of effective impurity concentration

The change of the effective impurity concentration due to radiation induced defects is derived from the depletion voltage via C–V measurements. As long as moderate neutron fluences are concerned the meas-

ured C–V characteristics are frequency independent indicating that the change of the depletion voltage is dominated by a corresponding change of the shallow dopant concentration only (dopant removal). After irradiation with high fluences ($\Phi > 10^{13}$ n/cm^2) a strong frequency dependence of the C–V curves is observed [8] in agreement with results reported by Kraner and Li [13,14]. In ref. [13] this effect is discussed in detail. In their model the depletion voltage is not only determined by shallow dopants but also by deep defect centers. The charge state of these centers depends on the position of the defect energy level with respect to the Fermi level in the band gap. The junction capacitance in the low frequency limit and at bias voltages larger than several volts can be approximated by:

$$C(V, \text{LF}) = \epsilon_{Si}\epsilon_0 \left(\frac{2\epsilon_{Si}\epsilon_0}{q_0 N_{eff}} V \right)^{-1/2} \qquad (1)$$

$N_{eff} = |N_d - N_t|$ is the compensated effective dopant concentration with $N_d = N_D - N_A$, N_D, N_A being the donor and acceptor density respectively and N_t is the concentration of the compensating deep trap level. It has been shown for many cases that the depletion voltage extracted from C–V characteristics is identical to that resulting from charge collection measurements performed with short ranged alpha particles [7,8].

In fig. 2 the absolute value of N_{eff} is plotted as function of the 1 MeV equivalent neutron fluence. For comparison we include the much smaller effect resulting from electron irradiation. The neutron data show a conduction type inversion at about 2×10^{12} n/cm^2 and a linear increase of an acceptor like defect concentration above 10^{13} n/cm^2 (see [5–8,15]). As discussed in a previous paper [8] the experimental results for neutron irradiation are corrected for all self annealing effects including those during and in between successive exposures. The used annealing function (eq. (1) of re. [8]) is demonstrated in fig. 3 together with measured values obtained for $\Phi < 5 \times 10^{12}$ n/cm^2. Our older results

Table 1
Parameters of the irradiation experiments

Radiation	E [MeV]	Hardness parameter κ	Intensity range [cm^{-2}s^{-1}] (Gy s^{-1})	Fluence (dose) range [cm^{-2}] (Gy)	Fluence (dose) error
Neutrons					
T (p, n)^{3}He [a]	1 2	0.88	7×10^6–1×10^7	7×10^{10}–1×10^{12}	4%
D (d, n)^{3}He [a]	5.0	1 69	1.5×10^7	4×10^{11}–2×10^{12}	3%
T (d, n)^{4}He [b]	14.1	1.88	1×10^6–6×10^8	1×10^9–3×10^{12}	5%
Be (d, n)B [a]	6.2	1.53	7×10^8–1×10^{10}	2×10^{10}–8×10^{14}	5%
Electrons [c]	1.8	$1 07 \times 10^{-2}$	1×10^{11}–3×10^{12} (28–843)	1×10^{12}–6×10^{15} (3×10^2 – 2×10^6)	2%

[a] Irradiation facilities at the Physikalisch-Technische-Bundesanstalt, Braunschweig.
[b] Irradiation facility at the University hospital, Hamburg
[c] Irradiation facility at the Telefunken System-Technik, Wedel.
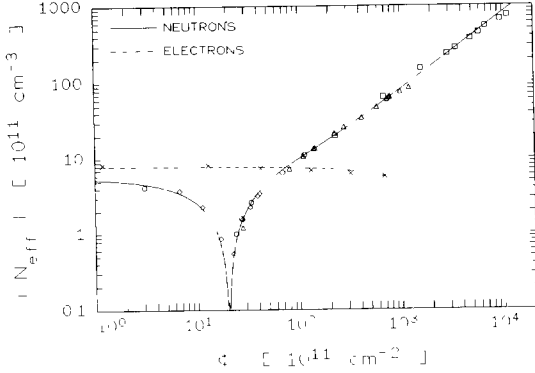
Fig. 2. Absolute value of the effective dopant concentration corrected for selfannealing versus normalized fluence for neutrons and electrons. The solid and dashed curves represent fits according to eq. (2).

Table 2

Time constants τ_i and relative amplitudes A_i for $\Delta N_{\text{eff}}(t)/\Delta N_{\text{eff}}(0)$ (eq. (1) in ref. [8]) obtained from fitting the data given in fig. 3

Time constants τ_i [min]	Relative amplitudes A_i
$(9.40) \pm 0.80 \times 10^{0}$	0.214 ± 0.030
$(6.87) \pm 0.14 \times 10^{1}$	0.262 ± 0.007
$(3.43) \pm 0.12 \times 10^{2}$	0.118 ± 0.008
$(4.00) \pm 0.04 \times 10^{3}$	0.097 ± 0.002
$(7.52) \pm 0.02 \times 10^{4}$	-0.107 ± 0.001
∞	0.417 ± 0.004

have now been extended to much larger annealing times up to 1 year, this way enabling us to derive the necessary predictions for real operational conditions in prospective LHC or SSC experiments [10]. A reanalysis of these data results in slightly changed parameters for the longest time constants. They are listed in table 2 (compare with table 2 of ref. [8]).

In modification of our previous empirical approach [8] we apply the following model for the fluence dependence of the effective dopant concentration. It is based on the fact that the annealing temperature of the vacancy–boron complex defect is only 270 K [16] and therefore a possible boron removal does not play a significant role for room temperature irradiation. In contrast donor removal due to the formation of E-centers (vacancy–phosphorus complex) is quite likely; this defect anneals out at about 420 K [17]. In addition

we have to assume the creation of acceptor like deep defect centers as before [8]. This leads finally to the following formula:

$$N_{\text{eff}}(\Phi) = N_{\text{D},0} \exp(-c\Phi) - (N_{\text{A},0} + b\Phi), \qquad (2)$$

where $N_{\text{D},0}$, $N_{\text{A},0}$ are the donor resp. acceptor concentrations before irradiation. This ansatz was proven to be correct for neutron irradiation by analyzing data derived at low and medium fluences for different detectors together with data of one detector irradiated up to 10^{14} n/cm^2. We chose only detectors with approximately the same initial effective donor concentration $N_{\text{D},0} - N_{\text{A},0}$ within a limit of 5%. Furthermore we supposed that the difference in the boron concentration of the individual detectors can be neglected. An estimate for $N_{\text{A},0}$ was achieved by an extrapolation of $N_{\text{eff}}(\Phi)$ values for fluences above 10^{13} n/cm^2 to $\Phi = 0$ (see eq. (2)). This results in a value of $N_{\text{A},0} = 2.4 \times 10^{11}$ cm^{-3}. A comparison between the experimental data and a fit according to eq. (2) with parameters $c_n = 3.5 \pm 0.2 \times 10^{-13}$ cm^2 and $b_n = 0.079 \pm 0.006$ cm^{-1} is shown in fig. 4. The acceptor creation parameter b_n is
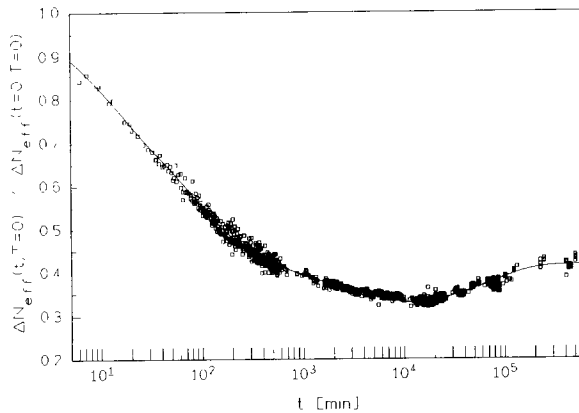

Fig. 3. Room temperature annealing data for the relative dopant concentration after neutron damage together with a fit (see text) and corresponding parameters given in table 2.
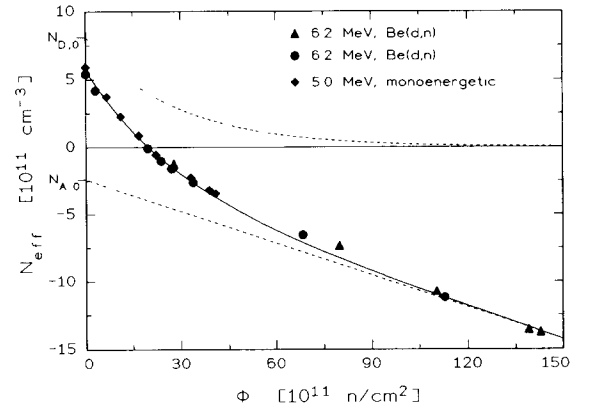

Fig. 4. Fluence dependence of the effective dopant concentration corrected for selfannealing. Solid curve: fit according to eq. (2); dashed lower and upper lines: acceptor creation resp. donor removal.

VIII. RADIATION DAMAGE

only slightly changed with respect to the previous publication [8], whereas the parameter c_n turns out to be lower by a factor of 2. It should be mentioned that the b-values presented in ref. [10] for n- and p-type material deviate from our value only by about 15%.

For electrons, using the same ansatz of eq. (2) and assuming the same boron concentration of $N_{A,0} = 2.4 \times 10^{11}$ cm ^{3} as obtained from the neutron irradiation data we get $c_e = 3.5 \pm 0.8 \times 10^{-15}$ cm^2 and $b_e = 0$. Although c_e is extracted with respect to the equivalent 1 MeV neutron fluence and therefore effects due to the different non-ionizing energy loss of electrons and neutrons are taken into account there is a very large remaining effect of $c_e/c_n \approx 10^{-2}$. This discrepancy indicates strong differences of the defect formation by neutrons and electrons. One reason may be attributed to a high recombination rate of primary defects (e.g. metastable closed pairs) induced by electrons. On the other hand the mean distance between the primary silicon interstitial and vacancy created by neutrons is much larger and hence a recombination is very unlikely [18].

It should be mentioned here that despite of the quite reassuring way of describing the effective dopant concentration as function of the neutron fluence we do not have a similarly consistent picture for the self annealing behaviour. In particular the reverse annealing at large time durations remains to be an open question.

4. Increase of reverse current

As reported in a previous paper [8] the $I–V$ characteristics at high neutron fluences above 10^{13} n/cm^2 saturate at a lower voltage than necessary for total depletion. On the other hand the current saturation voltage and the depletion voltage are identical at low fluences. As we are confident that the $C–V$ measurements reflect the real reach through of the electric field (see section 3) we are now plotting the detector current at this value as function of neutron fluence (fig. 5). Two fluence regions are obvious. Using the standard equation for the fluence dependence of the bulk current increase $\Delta I/V = \alpha \Phi$ we observe a damage coefficient of $\alpha_n = 8 \times 10^{-17}$ A/cm for $\Phi_n < 8 \times 10^{12}$ n/cm^2. Above a transition region related to type inversion α_n increases by a factor of about 2.5. Such behaviour was also observed for irradiations at $-20°C$ and for detectors fabricated by different technologies (see ref. [10]).

Again we include in fig. 5 results for electron irradiation using the normalization of the electron fluence as given in section 3. Here we derive a damage coefficient $\alpha_e = 4.2 \times 10^{-8}$ A/cm and hence $\alpha_e/\alpha_n \approx 0.05$ (α_n taken for low fluences). This ratio is therefore again
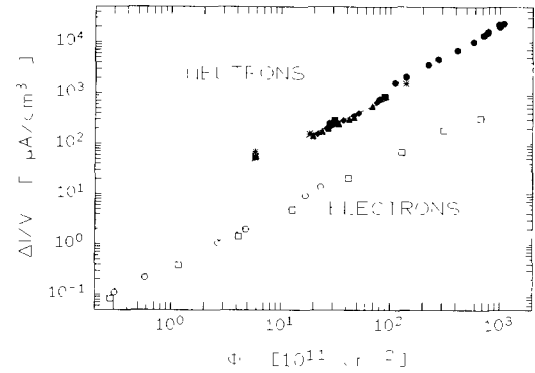

Fig. 5 Increase of measured reverse current at total depletion as function of normalized particle fluence for 6.2 MeV neutrons and 1 8 MeV electrons. Data corrected for self annealing.

much smaller than expected from the relative nonionizing energy loss alone. Van Lint [19] reported corresponding damage ratios for 3 MeV electrons (also with respect to 1 MeV neutrons) in low resistivity n-type material (1 and 10 Ω cm). Normalizing his data to 1.8 MeV electrons and extrapolating them with respect to the material resistivity a ratio of about 0.03 would be derived in good agreement with our own result.

All data plotted in fig. 5 are corrected for self annealing. The corresponding annealing functions are presented in fig. 6 for neutrons and electrons. The parameters of the applied formula (see ref. [8]) are listed in table 3. For neutron irradiated samples we observe again a different behaviour for low and high fluences respectively. Well above type inversion ($\Phi > 10^{13}$ n/cm^2) the amplitudes of the two short time constants are considerably larger than the values for low fluences. In addition a constant term is observed in contrast to the noninverted sample. These deviations may be due to surface effects concerning the change of the rectifying contact after inversion. The annealing effect for electron irradiated detectors is quite small compared to neutron irradiation. Only 40% of the initial current anneals out over a period of about 1 year.

5. Degradation of charge collection efficiency

Using short ranged monoenergetic alpha particles incident on the front and rear electrode of the detector it is possible to measure the charge collection efficiency resulting from the electron resp. hole contribution separately [4]. Measurements are performed as function of bias voltage above total depletion. Using the known drift velocities as function of electric field [20] we were able to extract the relevant trapping time
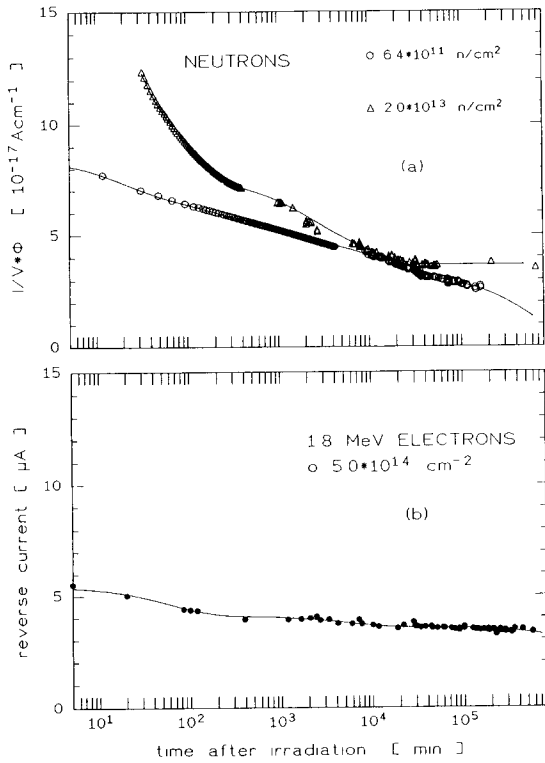
Fig. 6. Room temperature annealing of reverse current after 6.2 MeV neutron (a) and 1.8 MeV electron irradiation (b). The solid lines are fits to the data using parameters listed in table 3.

Fig. 7. Dependence of $1/\tau$ for electrons and holes on the normalized 1 MeV equivalent neutron fluence (see text).

constants for electrons and holes. These values are plotted as function of neutron fluence in fig. 7. For a given trap we expect $N_t \propto \Phi$. As $\tau \propto 1/N_t$ we would get a linear dependence of $1/\tau$ as function of Φ. For holes this expectation is confirmed in the full fluence range up to 2×10^{13} n/cm². However, for electrons a significant deviation from the initial slope is observed at 1×10^{13} n/cm². These measurements could not be carried out immediately after irradiation; appreciable
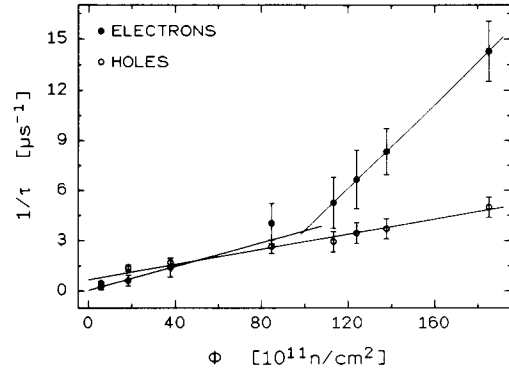
self annealing prior to the measurements could therefore not be avoided. Hence the onset of the increased electron trapping may be very well connected with type inversion to be expected at 2×10^{12} n/cm² immediately after irradiation and probably delayed here according to annealing [5]. Again this point needs further investigation. From fig. 7 we get

$$1/\tau = \gamma\Phi, \tag{3}$$

with $\gamma_h = 2.7 \times 10^{-7}$ cm²/s and $\gamma_e = 1.2 \times 10^{-6}$ cm²/s for $\Phi > 10^{13}$ n/cm². A detailed investigation with respect to the change of the internal electric field profile and trapping phenomena in neutron damaged detectors using the method of current pulse shape measurements is presented in the paper of Kraner et al. [21] at this conference. It is reassuring that both methods lead to approximately the same results.

From our τ-values we can deduce the resulting change in the charge collection for minimum ionizing particles. If we suppose e.g. an irradiation of 5×10^{13} n/cm² during a total exposure time of 10^7 s (1 equivalent operational year) leading to a depletion voltage of about 130 V for a 400 μm thick detector and if a bias voltage of 200 V is applied we get a charge collection deficiency of $\Delta Q/Q_0 = 12\%$ for mip's. This is in very

Table 3
Time constants τ_i and relative amplitudes A_i for the annealing of the bulk generation current obtained from fitting the data given in fig. 6

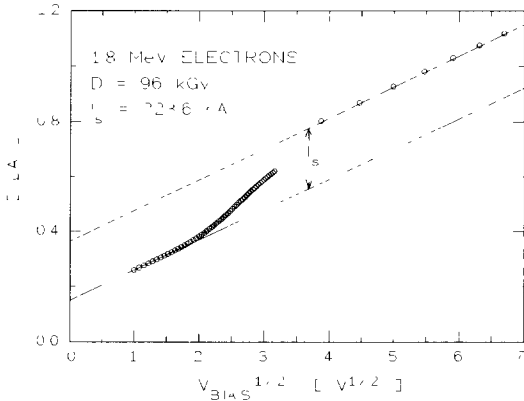| Neutrons: $\Phi = 6 \times 10^{11}$ n/cm²		Neutrons: $\Phi = 2 \times 10^{13}$ n/cm²		Electrons	
Time constant τ_i [min]	Relative amplitude A_i	Time constant τ_i [min]	Relative amplitude A_i	Time constant τ_i [min]	Relative amplitude A_i
1.78×10^1	0.16	1.29×10^1	0.20	6.2×10^1	0.25
1.19×10^2	0.11	8.54×10^1	0.30	5.5×10^3	0.10
1.09×10^3	0.13	1.83×10^3	0.13	7.0×10^6	0 65
1.47×10^4	0.20	9.50×10^3	0.13		
6.70×10^5	0.40	∞	0.24		

Fig. 8. Reverse current of an electron irradiated detector versus $V^{1/2}$ showing the oxide related surface contribution I_s (see text).

Fig. 10. Capacitance–voltage characteristics after damage by different electron dose values demonstrating the shift of the flat band voltage.

nice agreement with recent results reported by Lemeilleur et al. [15].

6. Surface effects

On top of the described bulk effects surface damage in the oxide passivation layers may be expected from ionizing radiation. Examples of such effects have been measured following electron irradiation and are shown in figs. 8–11. As discussed in detail in a previous paper the $I–V$ characteristic of our detectors is strongly influenced by the field plate overlapping the oxide edge [4]. At the onset of depletion underneath the field plate at about flat band voltage the SiO_2–Si interface states become active for carrier generation which is easily seen in a steep increase of the detector current. This effect is shown in fig. 8 for a detector irradiated with
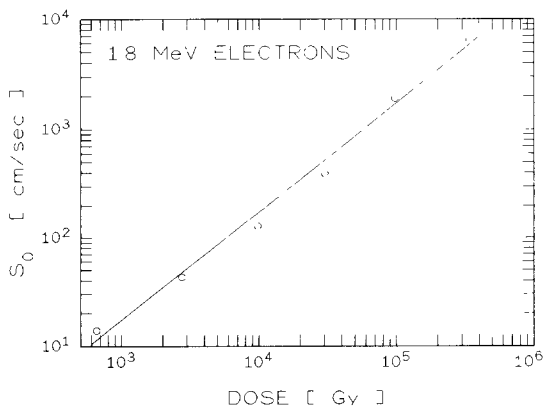
an electron dose of 96 kGy. Using the voltage dependence of the bulk generation current ($I \propto V$) we are able to extract the surface contribution only. This can be represented by the corresponding surface generation velocity:

$$S_0 = I_s/A_s q_0 n_i, \tag{4}$$

where I_s is the surface current related to the interface states, A_s the field plate area and n_i the intrinsic carrier density. We obtain an overall linear dependence as function of the electron dose (see fig. 9). This is in contrast to results of Snow et al. [22] which show a saturation above 0.1 MGy. The deviation may be due to a dose dependent lateral extension of the electric field beyond the geometrical limit of the field plate in our case. Therefore, according to an increase of A_s with fluence more interface states can contribute to the surface current.

Fig 9 Surface generation velocity S_0 (see eq. (4)) as function of absorbed electron dose. The solid line represents a mean slope of 0.017 cm/s Gy.
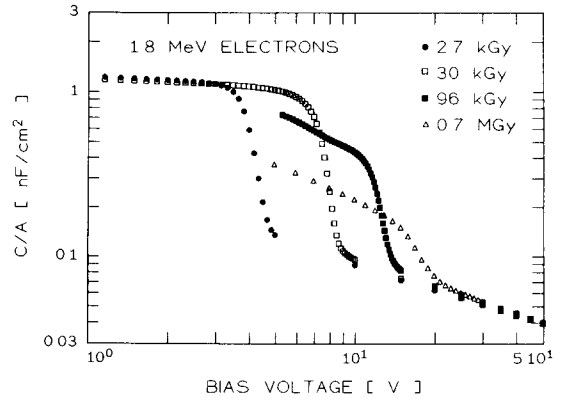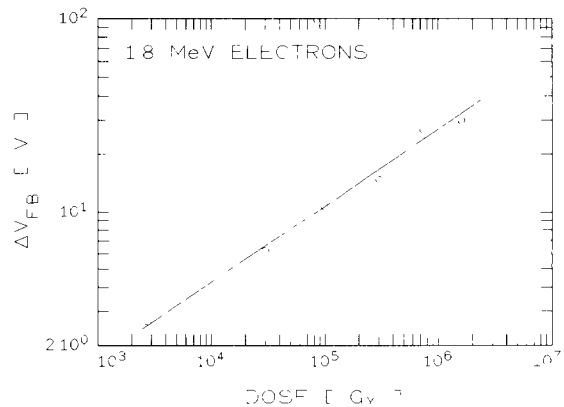

Fig. 11. Dependence of the flat band voltage shift on the electron radiation dose. The solid line corresponds to $\Delta V_{FB} \sim D^{0.4}$.

Another well known effect is the change of the flat band voltage originating from radiation induced trapped oxide charges and interface states (see e.g. ref. [23]). As an example in fig. 10 the change of the $C-V$ characteristic at low bias voltages with increasing electron dose is demonstrated. From the shift of the MOS related capacitance curves we deduced the change of the flat band voltage as function of electron dose (fig. 11). The measured values can be best represented by $\Delta V_{FB} \propto D^{0.4}$ (D being the absorbed dose). Such behaviour cannot be interpreted in a simple way as the trapped oxide charge as well as the charge of radiation induced interface traps depend in a complicated way on the transport phenomena of the created electron hole pairs in the oxide, the technology of the oxide growth and on further conditions during irradiation (see e.g. ref. [23]).

7. Conclusions

Our ongoing systematic studies of the radiation hardness of silicon detectors have been further complemented by a comparison of neutron and electron induced damage effects up to a fluence of 10^{15} n/cm^2 resp. a dose of 1 MGy. The results may be summarized as follows:

– The dependence of the effective dopant concentration as function of particle fluence can be well represented by a simple model taking donor removal and a fluence proportional creation of acceptor like states into account. Parameters for an appropriate function are derived. A neutron irradiation by 10^{14} n/cm^2 during an extended period of time, allowing for self annealing, would e.g. lead to a depletion voltage of only 140 V for 250 μm thick detectors. The donor removal due to electron irradiation is lower by a factor of 100 even if normalized to the same nonionizing energy loss. No acceptor creation is observed in this case.

– The bulk current increase is linear with respect to the particle fluence for both neutron and electron irradiation. The value of $\alpha_n = 8 \times 10^{-17}$ A cm^{-1} for neutrons is confirmed for fluences up to 10^{13} n/cm^2. The electron effect, normalized as above, is smaller by a factor of 20. Possibly due to surface effects the neutron related value α_n increases above type inversion by a factor of 2.5. After considerable self annealing this discrepancy is however strongly reduced again. Therefore it will not play a significant role for real operational conditions.

– Parameters for the charge collection efficiency have also been derived separately for the electron and hole contribution following neutron irradiations up to 2×10^{13} n/cm^2. Extrapolating these data to 10^{14} n/cm^2 we expect a signal pulse height degradation for mip's of less than 20% for 250 μm thick detectors biased at 200 V. Within the investigated electron fluence range no appreciable pulse degradation could be observed.

– Surface effects induced by electrons and attributed to the SiO$_2$ passivation layer as well as the SiO$_2$–Si interface are clearly visible and have been studied up to 1 MGy (100 Mrad). Even at this extremely high dose the observed effects are tolerable for safe detector operation. However an appreciable change may be expected if the detectors are irradiated under bias.

– Self annealing at room temperature has been studied in more detail up to 1 year after irradiation enabling us to predict the detector performance under real operational conditions. Although the self annealing functions for both the effective dopant concentration and the current increase can be well parametrized, using a set of exponentials, with different time constants and amplitudes no physical model for understanding the relevant effects can be presented so far.

References

[1] A. Ferrari, P.R. Sale, A. Fasso and G.R. Stevenson, EAGLE Internal Note, CAL-NO-005 (November 1991).

[2] M.S. Lazo, D.M. Woodall and P.J. McDaniel, Sandia Nat. Lab., Techn. report SAND87-0098, vol. 1 (1987).

[3] A. Van Ginneken, Fermi Nat. Acc. Lab., Report FN-522 (October 1989).

[4] E. Fretwurst, H. Herdan, G. Lindström, U. Pein, M. Rollwagen, H. Schatz, P. Thomsen and R. Wunstorf, Nucl. Instr. and Meth. A288 (1990) 1.

[5] G. Lindström, M. Eberle, I. Fedder, E. Fretwurst, U. Pein, V. Riech, H. Schatz, R. Wunstorf, C. Zeitnitz, N Croitoru, R. Darvas, A. Seidman, R Böttger and H. Schölermann in: Proc 5th Int. Conf. on Instrumentation for Colliding Beam Physics, Inst. of Nucl. Phys., Novosibirsk, 1990, ed. E.P. Solodov (World Scientific, Singapore, 1990) p. 331; and, DESY report, DESY 90-109 (September 1990).

[6] G. Lindström, M. Benkert, E. Fretwurst, T. Schulz, and R. Wunstorf in: Proc. Int. Conf. on Calorimetry in High Energy Physics, Fermilab, Batavia, 1990, eds. D.F. Andersen, M. Derrick, H.E. Fisk, A. Para and C.M. Sazana (World Scientific, Singapore, 1991) p. 467.

[7] R. Wunstorf, M. Benkert, E. Fretwurst, G. Lindström, T Schulz, N Croitoru, R. Darvas, M. Mudrik, R. Böttger and H. Schölermann, Nucl. Phys. B (Proc. Suppl.) 23A (1991) 324.

[8] R. Wunstorf, M. Benkert, N. Claussen, N. Croitoru, E. Fretwurst, G. Lindström and T. Schulz, Nucl. Instr. and Meth. A315 (1992) 149.

[9] G. Lindstrom, SITP internal report, SITP-TR-002, 1991, p. 1–11.

[10] SITP-Collaboration, Presented at 6th European Symp on Semiconductor Detectors, Milano, Italy, 1992.

[11] H.J Brede, G Dietze, K. Kodo, U.J. Schrewe, F Tancu and C Wen, Nucl. Instr. and Meth A274 (1989) 332; and,
H.J Brede, private communication

[12] T. Schulz, diploma thesis, University of Hamburg (1991).

[13] Z Li and H.W. Kraner, IEEE Trans. Nucl. Sci. NS-38(2) (1991) 244.

[14] Z Li, W. Chen and H.W. Kraner, Nucl. Instr. and Meth. A308 (1991) 585.

[15] F. Lemeilleur, M. Glaser, E H M. Heijne, P.Jarron and E. Occelli, IEEE Trans. Nucl. Sci NS-39(4) (1992) 551.

[16] G.D. Watkins, in: Deep Centers in Semiconductors, ed. S.T Pantelides (Gordon and Breach, New York, 1986) p 167

[17] L.C. Kimerling, H.M. DeAngelis and C.P. Carnes, Phys. Rev. B3 (1971) 427

[18] G.P Mueller and C.S. Guenzer, IEEE Trans. Nucl Sci. NS-27(6) (1980) 1474; and,
G.P Mueller, N D. Wilsey and M. Rosen, IEEE Trans. Nucl. Sci. NS-29 (6) (1982) 1493

[19] V.A.J. van Lint, T.M. Flanagan, R E. Leadon, J.A. Naber and V.C. Rogers, Mechanisms of Radiation Effects in Electronic Materials, vol. 1 (Wiley, New York, 1980).

[20] C Canalli and G. Ottaviani. J. Phys. Chem. Solids 32 (1971) 1707.

[21] H W. Kraner, E. Fretwurst and Z. Li, in these Proceedings (6th European Symp. on Semiconductor Detectors, Milano, Italy. 1992) Nucl. Instr. and Meth. A326 (1993) 350.

[22] E H. Snow, A.S Grove and D.J. Fitzgerald, Proc IEEE 55 (1967) 764

[23] J.R. Srour and M. McGarrity, Proc. IEEE 76 (11) (1988) 1443.